Nondisplaceable Binding Is a Potential Confounding Factor in ^{11}C-PBR28 Translocator Protein PET Studies

Gjertrud L. Laurell[1], Pontus Plavén-Sigray[1,2], Aurelija Jucaite[2,3], Andrea Varrone[2], Kelly P. Cosgrove[4,5], Claus Svarer[1], Gitte M. Knudsen[1,6], Karolinska Schizophrenia Project Consortium[7], R. Todd Ogden[8,9], Francesca Zanderigo[8,10], Simon Cervenka[2], Ansel T. Hillmer[4,5,11], and Martin Schain[1]

[1]Neurobiology Research Unit, Copenhagen University Hospital Rigshospitalet, Copenhagen, Denmark; [2]Centre for Psychiatry Research, Department of Clinical Neuroscience, Karolinska Institutet, and Stockholm Health Care Services, Region Stockholm, Stockholm, Sweden; [3]PET Science Centre, Precision Medicine and Genomics, R&D, AstraZeneca, Stockholm, Sweden; [4]PET Center, Department of Radiology and Biomedical Imaging, Yale University, New Haven, Connecticut; [5]Department of Psychiatry, Yale University, New Haven, Connecticut; [6]Faculty of Health and Medical Sciences, University of Copenhagen, Copenhagen, Denmark; [7]Karolinska Schizophrenia Project Consortium, Stockholm, Sweden; [8]Department of Biostatistics, Columbia University, New York, New York; [9]Molecular Imaging and Neuropathology Area, New York State Psychiatric Institute, New York, New York; [10]Department of Psychiatry, Columbia University College of Physicians and Surgeons, New York, New York; and [11]Department of Radiology and Biomedical Imaging, Yale University School of Medicine, New Haven, Connecticut

The PET ligand ^{11}C-PBR28 (*N*-((2-(methoxy-^{11}C)-phenyl)methyl)-*N*-(6-phenoxy-3-pyridinyl)acetamide) binds to the 18-kDa translocator protein (TSPO), a biomarker of glia. In clinical studies of TSPO, the ligand total distribution volume, V_T, is frequently the reported outcome measure. Since V_T is the sum of the ligand-specific distribution volume (V_S) and the nondisplaceable-binding distribution volume (V_{ND}), differences in V_{ND} across subjects and groups will have an impact on V_T. **Methods:** Here, we used a recently developed method for simultaneous estimation of V_{ND} (SIME) to disentangle contributions from V_{ND} and V_S. Data from 4 previously published ^{11}C-PBR28 PET studies were included: before and after a lipopolysaccharide challenge (8 subjects), in alcohol use disorder (14 patients, 15 controls), in first-episode psychosis (16 patients, 16 controls), and in Parkinson disease (16 patients, 16 controls). In each dataset, regional V_T estimates were obtained with a standard 2-tissue-compartment model, and brain-wide V_{ND} was estimated with SIME. V_S was then calculated as $V_T - V_{ND}$. V_{ND} and V_S were then compared across groups, within each dataset. **Results:** A lower V_{ND} was found for individuals with alcohol-use disorder (34%, $P = 0.00084$) and Parkinson disease (34%, $P = 0.0032$) than in their corresponding controls. We found no difference in V_{ND} between first-episode psychosis patients and their controls, and the administration of lipopolysaccharide did not change V_{ND}. **Conclusion:** Our findings suggest that in TSPO PET studies, nondisplaceable binding can differ between patient groups and conditions and should therefore be considered.

Key Words: PET; translocator protein; ^{11}C-PBR28; simultaneous estimation; kinetic modeling

J Nucl Med 2021; 62:412–417
DOI: 10.2967/jnumed.120.243717

PET with radioligands for the glial marker 18-kDa translocator protein (TSPO) has been extensively used over the past 2 decades to assess brain immune function in vivo (*1*). ^{11}C-PBR28 (*N*-((2-(methoxy-^{11}C)-phenyl)methyl)-*N*-(6-phenoxy-3-pyridinyl)acetamide) is a second-generation TSPO radioligand with signal-to-noise characteristics superior to those of the first-generation radioligand ^{11}C-PK11195 (*2*). As with other second-generation TSPO tracers, the affinity of ^{11}C-PBR28 to TSPO is affected by a single-nucleotide polymorphism on the TSPO gene (rs6971), and in clinical studies, TSPO genotype is used to classify subjects as low-, mixed-, or high-affinity binders (*3,4*).

PET ligand binding to TSPO is often quantified by fitting a 2-tissue-compartment model (2TCM), or variants thereof (*5*), to the PET time–activity curves, using parent radioligand concentration in arterial plasma as the input function. The 2TCM describes the ligand kinetics using 2 tissue compartments, one for ligand that is bound specifically to the target of interest and one for nondisplaceable binding. The nondisplaceable compartment includes both free and nonspecifically bound radioligand. The standard outcome measure reported using 2TCM is the total distribution volume (V_T), which represents the ratio of total activity concentration in tissue to that in plasma at equilibrium. V_T is the sum of the nondisplaceable and specific distribution volumes ($V_T = V_{ND} + V_S$). Some radioligands display negligible specific binding in a certain brain region (i.e., $V_S = 0$). Such a region is usually referred to as a reference region and can be used to estimate V_{ND}, which is assumed to be constant throughout the brain. When a reference region is available, the binding potential with nondisplaceable uptake as a reference, BP_{ND} ($=V_S/V_{ND}$), is typically the reported

Received Feb. 17, 2020; revision accepted Jun. 23, 2020.
For correspondence or reprints contact: Gjertrud L. Laurell, Neurobiology Research Unit, Rigshospitalet, Blegdamsvej 9, DK-2100, Copenhagen, Denmark.
E-mail: gjertrud.laurell@nru.dk
Published online Jul. 17, 2020.
COPYRIGHT © 2021 by the Society of Nuclear Medicine and Molecular Imaging.

outcome measure. TSPO is expressed throughout the brain, and thus, no reference region exists for this target. It is therefore challenging to obtain reliable estimates of the relative contributions from the specific and nondisplaceable binding, leaving a degree of uncertainty about the interpretation of V_T.

Recently, a method for simultaneous estimation of V_{ND} (SIME) (*6*) was developed to estimate V_{ND} for tracers without a reference region. SIME uses the assumption that nondisplaceable binding is constant throughout the brain and estimates a global value for V_{ND} by fitting a constrained 2TCM for several brain regions simultaneously. The performance of SIME with ^{11}CPBR28 has been thoroughly tested in healthy human subjects (*7*). Using simulations, pharmacologic competition data, and test–retest data, SIME-derived estimates of V_{ND} and V_S (calculated using 2TCM V_T and SIME V_{ND}) were shown to be accurate and reliable (*7*).

For comparison of V_T between groups to be meaningful, there must be an underlying assumption that V_{ND} is the same across the groups. Currently, there is limited scientific evidence to back up this assumption. Hence, our aim with this study was to investigate whether nondisplaceable binding can be a confounding factor in TSPO PET studies that use V_T as an outcome measure. To achieve this aim, SIME was used to quantify V_{ND} in ^{11}C-PBR28 data from 4 different published datasets. In the first dataset, an immune stimulator was administered to healthy subjects (*8*). The 3 remaining datasets contain controls and subjects with alcohol-use disorder (AUD) (*9*), first-episode psychosis (FEP) (*10*), and Parkinson disease (PD) (*11*).

MATERIALS AND METHODS

This study includes 4 datasets obtained at 2 PET centers. All subjects underwent a ^{11}C-PBR28 PET scan in a high-resolution research tomograph (Siemens). Metabolite-corrected arterial input functions were collected for all scans. T1-weighted MRI scans were acquired to define regions of interest (ROIs). All subjects were genotyped for the rs6971 polymorphism, and low-affinity binders were excluded. In previous publications, V_T has been the primary reported outcome measure. A list of the datasets, with subject information, is reported in Table 1, and the reader is referred to the original publications for further details on data acquisition and processing.

Lipopolysaccharide

The lipopolysaccharide dataset (*8*) was collected at the Yale PET Center. Eight healthy men were scanned twice on the same day, at baseline and 3 h after injection of lipopolysaccharide (dose 1.0 ng/kg), an acute immune stimulus. ^{11}C-PBR28 was injected as a 1-min bolus, and the PET scan duration was 120 min.

AUD

The AUD dataset (*9*) was collected at the Yale PET center. It consists of 14 subjects with AUD and 15 age-matched control subjects. Five of the control subjects also participated in the lipopolysaccharide experiment. AUD subjects were imaged 1–4 d (in 1 case, 24 d) after intake of their last alcoholic beverage. ^{11}C-PBR28 was injected as a 1-min bolus, and the PET scan duration was 120 min.

FEP

The FEP dataset (*10*) was collected at Karolinska Institutet. It consists of 16 FEP patients and 16 age-matched controls. All patients were naïve to antipsychotic drugs. ^{11}C-PBR28 was injected as a 10-s bolus, and the PET scan duration was approximately 90 min.

PD

The PD dataset (*11*) was collected at Karolinska Institutet. It consists of 16 patients with PD and 16 age-matched controls. ^{11}C-PBR28 was injected as a 10-s bolus, and the PET scan duration was 72 min.

SIME

The SIME method (*6*) works by first defining a grid of possible V_{ND} values. Then, for each value in the grid, a 2TCM is fitted to the time–activity curves with the constraint that $K_1 = V_{ND} \cdot k_2$ in all ROIs, reducing the number of rate constants from 4 to 3. The residual sum of squares is then computed for all ROIs and frames, and the V_{ND} that yields the lowest residual sum of squares is selected as the estimate of a brain-wide V_{ND}.

TABLE 1
Dataset Summary

Dataset	Group	Subjects (*n*)		Age	
		HABs	MABs	HABs	MABs
Sandiego, 2015	Lipopolysaccharide	3	5	28.0 ± 6.0 (22.7–34.5)	23.6 ± 5.1 (19.1–31.1)
Hillmer, 2017	AUD				
	Controls	8	7	37.4 ± 9.0 (26.3–48.4)	32.8 ± 14.6 (19.1–55.6)
	Patients	7	7	40.9 ± 7.9 (31.6–55.2)	37.9 ± 10.4 (26.9–51.0)
Collste, 2017	FEP				
	Controls	9	7	27.8 ± 9.3 (22–50)	25.7 ± 8.2 (20–43)
	Patients	6	10	29.8 ± 8.2 (20–40)	27.7 ± 8.8 (19–47)
Varnäs, 2019	PD				
	Controls	8	8	64.9 ± 4.9 (57.8–71.5)	62.1 ± 5.3 (56.1–72.0)
	Patients	8	8	63.6 ± 4.3 (57.1–69.1)	63.4 ± 6.4 (55.2–73.2)

HAB = high-affinity binder; MAB = mixed-affinity binder.
Age is given as mean ± SD, followed by range in parentheses.

For all datasets, we used a V_{ND} grid from 0.01 to 5, with steps of 0.01, based on previous studies with SIME and ^{11}C-PBR28 (*7,12*). Initial evaluation of the data indicated that this range covers the cost function minimum. The residual sum of squares was weighted by the square root of the frame duration. Fractional blood volume was fitted for each ROI separately. SIME V_{ND} was calculated using time–activity curves from the cerebellum, parietal cortex, frontal cortex, occipital cortex, temporal cortex, putamen, caudate, and thalamus, thus covering various brain structures and tissue types.

Calculation of Outcome Measures and ROIs

In each ROI, V_T was calculated using a standard 2TCM, including fitting of the fractional blood volume. V_S ($=V_T - V_{ND}$) was calculated from the 2TCM V_T estimates and the SIME V_{ND} estimates. For all datasets except the PD dataset, we report ROI-specific outcome measures (V_T, V_S) in the cerebellum and frontal cortex. For PD, we report V_T and V_S in the striatum instead of the frontal cortex, because the striatum is considered a key region in the pathophysiology of PD and is more frequently reported in PET studies.

Statistical Analysis

Statistical analyses were performed using MATLAB (version 9.5; MathWorks). For the lipopolysaccharide data, a paired-sample *t* test was used for all outcome measures (V_{ND}, V_T, and V_S) to test for a difference between the pre- and postlipopolysaccharide scans. The percentage change in the outcome measures for each subject was calculated as 100·(pre − post)/pre. For the remaining datasets, a univariate 2-way ANOVA without an interaction term was applied for each outcome measure (V_{ND}, V_T, and V_S) to determine the group differences between controls and patients, with log-transformed outcome measures as a dependent variable and diagnosis and genotype as fixed factors, as described earlier (*12*). Using the regression coefficients, β, from the ANOVA, the percentage difference between patients and controls across genotypes was calculated as $100 \cdot (e^{\beta_{patient} - \beta_{control}} - 1)$. The α-level was set to 0.05. Reported *P* values were not corrected for multiple comparisons.

RESULTS

For all datasets, the results obtained for V_T are in accordance with those in the original publications. Below, we report the results for V_T, V_S, and V_{ND} for each dataset separately. The results for the ROIs presented below are consistent with the remaining ROIs included in the SIME calculation (Supplemental Tables 1–4; supplemental materials are available at http://jnm.snmjournals.org). Results were also unchanged when an interaction term was included in the ANOVA (Supplemental Tables 5–7) and when volume-based weights were used in the SIME analysis (Supplemental Tables 8–11).

Lipopolysaccharide

Lipopolysaccharide injection was associated with a significant increase in V_T in both the cerebellum (mean, 40% [SD, 34%]; $P = 0.016$) and the frontal cortex (mean, 46% [SD, 23%]; $P = 0.0012$). V_{ND} was not affected by lipopolysaccharide (mean, 15% [SD, 40%]; $P = 0.38$). The mean increase in V_S was 59% (SD, 51%) ($P = 0.0052$) in the cerebellum and 66% (SD, 35%) ($P = 0.00026$) in the frontal cortex. The results are summarized in Figure 1.

AUD

V_T was significantly lower in AUD subjects than in controls, both in the cerebellum (18%, $P = 0.012$) and in the frontal cortex (23%, $P = 0.0048$). V_{ND} was 34% lower in patients than in controls ($P = 0.00084$). V_S did not differ significantly between the groups. These results are shown in Figure 2. Genotype had a significant effect on both V_T and V_S ($P < 0.0005$) but not on V_{ND}.

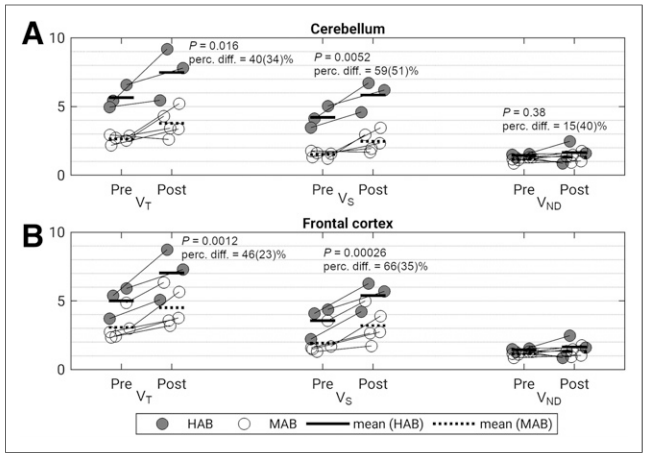

FIGURE 1. Change in outcome measures (V_T, V_S, and V_{ND}) between pre- and postlipopolysaccharide scans in cerebellum (A) and frontal cortex (B). Individual subjects are connected with a line. *P* values and percentage difference (perc. diff.) between pre- and postlipopolysaccharide scans are shown. HAB = high-affinity binder; MAB = mixed-affinity binder.

FEP

In the FEP dataset, V_T was overall lower in patients than in controls (32%, $P = 0.060$ in the cerebellum; 36%, $P = 0.045$ in the frontal cortex). There was no significant difference in V_{ND} between patients and controls ($P = 0.30$). V_S exhibited a larger percentage separation between patients and controls than that observed for V_T in both the cerebellum (44%, $P = 0.054$) and the frontal cortex (57%, $P = 0.033$). The results are shown in Figure 3. The effect of genotype was statistically significant for V_T in the cerebellum and frontal cortex ($P = 0.011$ and 0.017, respectively), for V_{ND} in the ■■■ ($P = 0.0043$), and for V_S in the frontal cortex ($P = 0.017$) but not in the cerebellum ($P = 0.099$).

PD

In the PD dataset, we found no statistically significant difference in V_T or V_S between patients and controls, in either the cerebellum ($P = 0.74$ for V_T, $P = 0.11$ for V_S) or the striatum ($P = 0.32$ for V_T, $P = 0.42$ for V_S). V_{ND} was, however, lower in patients than in

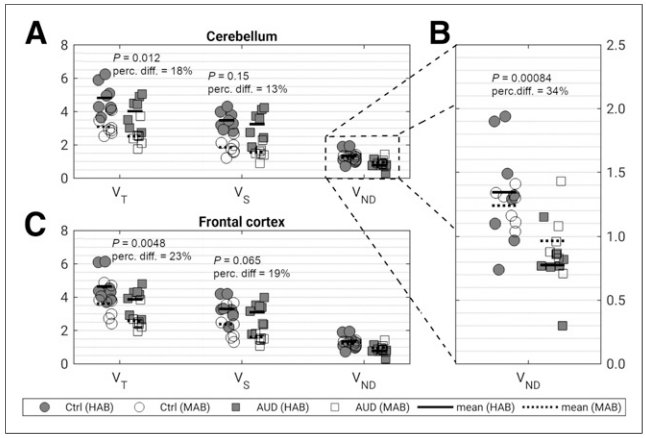

FIGURE 2. (A and C) Difference in outcome measures (V_T, V_S, and V_{ND}) between controls (Ctrl) and subjects with AUD in cerebellum (A) and frontal cortex (C). (B) Zoomed view of results for V_{ND}. *P* values and percentage difference (perc. diff.) between controls and patients are shown. HAB = high-affinity binder; MAB = mixed-affinity binder.

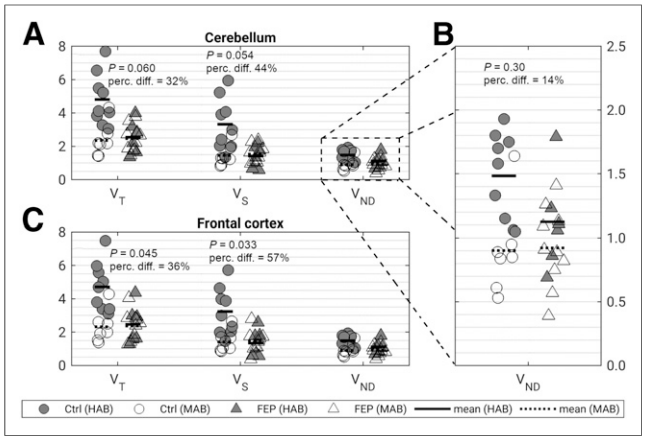

FIGURE 3. (A and C) Difference in outcome measures (V_T, V_S, and V_{ND}) between controls (Ctrl) and FEP patients in cerebellum (A) and frontal cortex (C). (B) Zoomed view of results for V_{ND}. *P* values and percentage difference (perc. diff.) between controls and patients are shown. HAB = high-affinity binder; MAB = mixed-affinity binder.

controls (34%, $P = 0.0032$). These results are shown in Figure 4. Across all outcome measures and ROIs, there was a significant effect of genotype ($P = 0.012$ for V_{ND}, $P < 10^{-6}$ for V_T and V_S).

DISCUSSION

In this study, we used a new method to estimate V_{ND} in 4 clinical ^{11}C-PBR28 datasets. We found that V_{ND} estimated with this method was lower in AUD and PD than in their matched controls, whereas no difference was found between FEP patients and their controls or in subjects before and after lipopolysaccharide injection. This was, to our knowledge, the first attempt to disentangle the extent by which differences in nondisplaceable binding may contribute to the observed differences in V_T.

Lipopolysaccharide

Although leading to a pronounced increase in V_T, administration of lipopolysaccharide had no apparent effect on SIME V_{ND}. Lipopolysaccharide is a useful model to study an acute immune response, and upregulation of TSPO has been observed in vivo in several species, including mice (*13*), rats (*14*), pigs (*15*), and nonhuman primates (*16*). When using V_S as an outcome measure, we observed a larger percentage separation between the pre- and postlipopolysaccharide scans, with mean differences of 59% and 66% in the cerebellum and frontal cortex, respectively, and with variability similar to that of V_T (coefficient of variation [SD/mean] was 0.85 for V_T and 0.86 for V_S). This higher percentage difference occurred because V_{ND} is not affected by the challenge. In a scenario in which V_{ND} is unaffected by a particular disease, and V_T consists of one third of V_{ND} and two thirds of V_S, a 50% difference in specific TSPO binding translates to only a 33% difference in V_T. In such a scenario, though the effect sizes might likely be the same, it follows that changes in V_S more directly reflect changes in TSPO densities, whereas changes in V_T are attenuated by the contribution from V_{ND}.

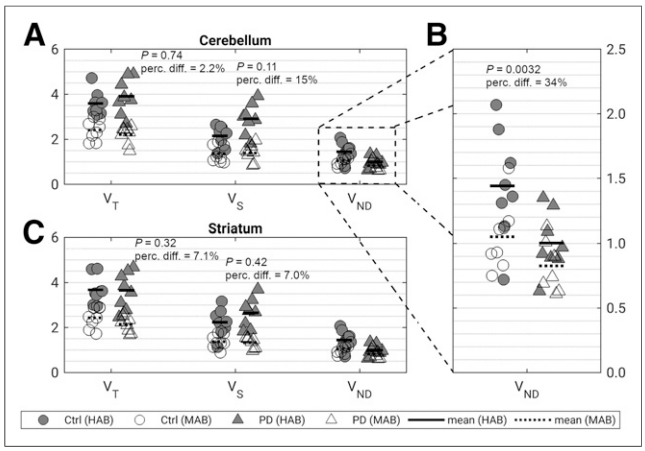

FIGURE 4. (A and C) Difference in outcome measures (V_T, V_S, and V_{ND}) between controls (Ctrl) and PD patients in cerebellum (A) and striatum (C). (B) Zoomed view of results for V_{ND}. *P* values and percentage difference (perc. diff.) between controls and patients are shown. HAB = high-affinity binder; MAB = mixed-affinity binder.

AUD

Both V_T and V_{ND} were lower in AUD subjects than in their age-matched controls, with a similar trend in V_S. This finding may explain a previous report in which mixed-affinity binders with AUD had a lower ^{11}C-PBR28 V_T than mixed-affinity binder controls across several brain regions, whereas no difference was seen in high-affinity binders (*17*), since V_{ND} composes a larger fraction of V_T in mixed-affinity binders than in high-affinity binders. In a separate cohort, Kalk et al. reported a lower ^{11}C-PBR28 hippocampal V_T in alcohol-dependent subjects than in controls, across both genotypes (*18*). In the present analysis, although some of the differences in V_T between AUD and controls were ascribed to differences in V_{ND}, frontal cortex V_S still showed a sizeable (albeit nonsignificant) percentage difference between AUD subjects and their controls. We can only speculate why V_{ND} would be lower in AUD subjects; pharmacologic competition studies in this population would be needed to conclusively establish levels of specific and nondisplaceable radiotracer uptake. Chronic alcohol exposure induces brain tissue atrophy, reduces cerebral perfusion, and accelerates aging (*19,20*). Including gray matter volume as a covariate in the statistical analysis did not change the results, indicating that the findings are not driven by partial-volume effects (Supplemental Table 12). Age-related alterations in tissue composition have been proposed as an explanation for differences in V_{ND} observed with the 5-hydroxytryptamine receptor 2A ligand ^{18}F-altanserin (*21*). Although these questions remain unanswered, the findings here reported illustrate how separation of V_{ND} and V_S could change the interpretation of results from TSPO PET studies.

FEP

Patients with FEP had SIME V_{ND} estimates similar to those of their matched controls. Frontal cortex V_T and V_S values were lower in patients. Using V_S as an outcome measure resulted in a larger percentage difference between the groups. Most previous TSPO PET studies of FEP and schizophrenia have found no significant differences in V_T (*22–24*), whereas a recent metaanalysis, which pooled PET data from 5 studies on psychosis and schizophrenia using second-generation TSPO radioligands (152 subjects in total), found strong evidence for lower V_T values in patients than in controls (*25*). If V_S had been used as the outcome measure in previous TSPO PET studies of FEP and schizophrenia, it is possible that the power to detect the population effect of a lower TSPO also in the individual samples of patients would have been higher.

PD

We found that SIME V_{ND} was lower in PD patients than in controls, but we observed no significant differences in V_T, consistent with findings in TSPO PET studies using another second-generation radioligand (*26,27*). One study, using ^{11}C-PK11195 and a basis-function implementation of the simplified reference tissue model, found a higher BP_{ND} in PD patients than in controls (*28*). Since BP_{ND} is defined as V_S/V_{ND}, and given our findings, it is possible that the higher BP_{ND} reported in the ^{11}C-PK11195 study was due to lower nondisplaceable binding rather than higher specific binding. This possibility illustrates that V_{ND} is a potential confounding factor not only in studies using V_T as an outcome measure but also in those reporting BP_{ND}. By using ratio-based methods to provide BP_{ND} in TSPO PET studies, one may mistakenly interpret a decrease in V_{ND} as an increase in TSPO binding. Similar to the finding in the AUD dataset, PD might be associated with increased global atrophy (*29*), and it is possible that altered tissue composition could explain the lower V_{ND} in PD patients. Further studies are required to establish the reason for this observed group difference.

Effect of V_{ND} on Genotype

We observed a pronounced effect of genotype on SIME V_{ND} in both the FEP and the PD datasets but not in the AUD data. The observed effect, if true, complicates interpretation of our current understanding of the TSPO polymorphism, by implicating effects both on the tracer's affinity to TSPO and on nondisplaceable uptake. When all the controls in this study were pooled, a difference in V_{ND} between genotypes was quite evident ($P = 0.00016$). We identify 3 potential interpretations for this observation. One possibility is that SIME-derived estimates of V_{ND} are artefactually contaminated by estimates of V_S, so that high specific binding results in an overestimation of V_{ND}. However, this spillover across compartments has previously been tested and discarded using simulations (*7*). This finding is also supported by the lipopolysaccharide experiment, in which increased V_S is not reflected in V_{ND}. A second interpretation is that the higher affinity of the radioligand in high-affinity binders leads to a higher nondisplaceable binding because equilibrium conditions are achieved at a later time for a high-affinity versus a low-affinity radioligand. The same mechanisms could potentially lead to higher nondisplaceable tracer binding in high-target-density brain regions than in regions with low target densities. For ^{11}C-raclopride, it has been suggested that regional differences in observed occupancy could in fact be attributable to spatially varying nondisplaceable uptake (*30,31*). The third possibility is that SIME-derived V_{ND} estimates are affected by other features, which are, in turn, dependent on the genotype. For instance, it has previously been shown that V_{ND} estimated with SIME may be sensitive to the shapes of the arterial input function (*32*). The fact that input functions may differ between genotypes has been shown for both ^{11}C-PBR28 (*7*) and the TSPO SPECT radioligand ^{123}I-CLINDE (*33*), as is to be expected from the different levels of binding to TSPO in peripheral tissue (*34*). Irrespective of cause, estimates of V_{ND} (and, as a consequence, of BP_{ND}) may not be directly comparable across genotype groups, and their difference could itself be a confounder in clinical studies if the cohort is not balanced across genotypes. The datasets included in this study, however, are well balanced across genotypes; as such, a potential influence of differences in V_{ND} estimates is unlikely. Pharmacologic competition data would be needed to conclusively establish any effect of genotype on V_{ND}. However, previous ^{11}C-PBR28 blocking studies have included only high-affinity-binder individuals (*35*) and therefore cannot provide insights into potential differences between genotypes.

Limitations

For any arterial input model, including SIME, V_{ND} estimates are sensitive to the input function shape. Further, similar to reference-tissue modeling, we did not consider spatial variations in V_{ND}. SIME was additionally executed on a larger set of ROIs, which resulted in close-to-identical findings (Supplemental Table 13). Yet, a formal procedure on how to establish a suitable ROI set for estimation of V_{ND} remains to be investigated.

CONCLUSION

Our findings suggest that V_{ND} may be a potential confounding factor in ^{11}C-PBR28 PET studies. This outcome warrants further studies to establish the observed V_{ND} differences and, if possible, reveal their causes. We recommend the use of V_S as an additional outcome parameter in TSPO PET studies since this measure more directly reflects binding to TSPO.

DISCLOSURE

Martin Schain was supported by a NARSAD young investigator grant from the Brain & Behavior Research Foundation. Pontus Plavén-Sigray was supported by the Lundbeck Foundation and the Swedish Society for Medical Research. Ansel Hillmer was supported by NIH grant K01AA024788. Simon Cervenka was supported by Swedish Research Council grant 523-2014-3467. No other potential conflict of interest relevant to this article was reported.

ACKNOWLEDGMENTS

The Karolinska Schizophrenia Project consortium consists of Lars Farde, Lena Flyckt, Göran Engberg, Sophie Erhardt, Helena Fatouros-Bergmann, Simon Cervenka, Lilly Schwieler, Fredrik Piehl, Ingrid Agartz, Karin Collste, Pauliina Victorsson, Anna Malmqvist, Mikael Hedberg, and Funda Orhan.

KEY POINTS

QUESTION: Is nondisplaceable binding a confounding factor in ^{11}C-PBR28 PET studies?

PERTINENT FINDINGS: Nondisplaceable uptake was estimated for 4 ^{11}C-PBR28 PET datasets. In 2 of these (AUD and PD) there was a significant difference in nondisplaceable uptake between patients and controls.

IMPLICATIONS FOR PATIENT CARE: The possibility of obtaining estimates of specific binding to TSPO may improve the interpretability of nuclear imaging studies addressing the role of neuroinflammation in several disorders.

REFERENCES

1. Liu GJ, Middleton RJ, Hatty CR, et al. The 18 kDa translocator protein, microglia and neuroinflammation. *Brain Pathol.* 2014;24:631–653.
2. Fujita M, Kobayashi M, Ikawa M, et al. Comparison of four ^{11}C-labeled PET ligands to quantify translocator protein 18 kDa (TSPO) in human brain: (*R*)-PK11195, PBR28, DPA-713, and ER176-based on recent publications that measured specific-to-non-displaceable ratios. *EJNMMI Res.* 2017;7:84.

3. Owen DR, Howell OW, Tang S-P, et al. Two binding sites for [^{3}H]PBR28 in human brain: implications for TSPO PET imaging of neuroinflammation. *J Cereb Blood Flow Metab.* 2010;30:1608–1618.
4. Owen DR, Yeo AJ, Gunn RN, et al. An 18-kDa translocator protein (TSPO) polymorphism explains differences in binding affinity of the PET radioligand PBR28. *J Cereb Blood Flow Metab.* 2012;32:1–5.
5. Rizzo G, Veronese M, Tonietto M, Zanotti-Fregonara P, Turkheimer FE, Bertoldo A. Kinetic modeling without accounting for the vascular component impairs the quantification of [^{11}C]PBR28 brain PET data. *J Cereb Blood Flow Metab.* 2014;34:1060–1069.
6. Ogden RT, Zanderigo F, Parsey RV. Estimation of in vivo nonspecific binding in positron emission tomography studies without requiring a reference region. *Neuroimage.* 2015;108:234–242.
7. Plavén-Sigray P, Schain M, Zanderigo F, et al. Accuracy and reliability of [^{11}C] PBR28 specific binding estimated without the use of a reference region. *Neuroimage.* 2019;188:102–110.
8. Sandiego CM, Gallezot J-D, Pittman B, et al. Imaging robust microglial activation after lipopolysaccharide administration in humans with PET. *Proc Natl Acad Sci USA.* 2015;112:12468–12473.
9. Hillmer AT, Sandiego CM, Hannestad J, et al. In vivo imaging of translocator protein, a marker of activated microglia, in alcohol dependence. *Mol Psychiatry.* 2017;22:1759–1766.
10. Collste K, Plavén-Sigray P, Fatouros-Bergman H, et al. Lower levels of the glial cell marker TSPO in drug-naive first-episode psychosis patients as measured using PET and [^{11}C]PBR28. *Mol Psychiatry.* 2017;22:850–856.
11. Varnäs K, Cselényi Z, Jucaite A, et al. PET imaging of [^{11}C]PBR28 in Parkinson's disease patients does not indicate increased binding to TSPO despite reduced dopamine transporter binding. *Eur J Nucl Med Mol Imaging.* 2019;46: 367–375.
12. Schain M, Zanderigo F, Ogden RT, Kreisl WC. Non-invasive estimation of [^{11}C] PBR28 binding potential. *Neuroimage.* 2018;169:278–285.
13. Vignal N, Cisternino S, Rizzo-Padoin N, et al. [^{18}F]FEPPA a TSPO radioligand: optimized radiosynthesis and evaluation as a PET radiotracer for brain inflammation in a peripheral LPS-injected mouse model. *Molecules.* 2018;23:1375.
14. Dickens AM, Vainio S, Marjamäki P, et al. Detection of microglial activation in an acute model of neuroinflammation using PET and radiotracers ^{11}C-(*R*)-PK11195 and ^{18}F-GE-180. *J Nucl Med.* 2014;55:466–472.
15. de Lange C, Solberg R, Holtedahl JE, et al. Dynamic TSPO-PET for assessing early effects of cerebral hypoxia and resuscitation in new born pigs. *Nucl Med Biol.* 2018;66:49–57.
16. Hillmer AT, Holden D, Fowles K, et al. Microglial depletion and activation: A [^{11}C]PBR28 PET study in nonhuman primates. *EJNMMI Res.* 2017;7:59.
17. Kim SW, Wiers CE, Tyler R, et al. Influence of alcoholism and cholesterol on TSPO binding in brain: PET [^{11}C]PBR28 studies in humans and rodents. *Neuropsychopharmacology.* 2018;43:1832–1839.
18. Kalk NJ, Guo Q, Owen D, et al. Decreased hippocampal translocator protein (18 kDa) expression in alcohol dependence: a [^{11}C]PBR28 PET study. *Transl Psychiatry.* 2017;7:e996.
19. Oscar-Berman M, Valmas MM, Sawyer KS, Ruiz SM, Luhar RB, Gravitz ZR. Profiles of impaired, spared, and recovered neuropsychologic processes in alcoholism. *Handb Clin Neurol.* 2014;125:183–210.
20. Luo A, Jung J, Longley M, et al. Epigenetic aging is accelerated in alcohol use disorder and regulated by genetic variation in APOL2. *Neuropsychopharmacology.* 2020;45:327–336.
21. Adams KH, Pinborg LH, Svarer C, et al. A database of [^{18}F]-altanserin binding to 5-HT2A receptors in normal volunteers: normative data and relationship to physiological and demographic variables. *Neuroimage.* 2004;21:1105–1113.
22. Bloomfield PS, Selvaraj S, Veronese M, et al. Microglial activity in people at ultra high risk of psychosis and in schizophrenia: an [^{11}C]PBR28 PET brain imaging study. *Am J Psychiatry.* 2016;173:44–52.
23. Kenk M, Selvanathan T, Rao N, et al. Imaging neuroinflammation in gray and white matter in schizophrenia: an in-vivo PET study with [^{18}F]-FEPPA. *Schizophr Bull.* 2015;41:85–93.
24. Hafizi S, Tseng H-H, Rao N, et al. Imaging microglial activation in untreated first-episode psychosis: a PET study with [^{18}F]FEPPA. *Am J Psychiatry.* 2017;174:118–124.
25. Plavén-Sigray P, Matheson GJ, Collste K, et al. Positron emission tomography studies of the glial cell marker translocator protein in patients with psychosis: a meta-analysis using individual participant data. *Biol Psychiatry.* 2018;84:433–442.
26. Ghadery C, Koshimori Y, Coakeley S, et al. Microglial activation in Parkinson's disease using [^{18}F]-FEPPA. *J Neuroinflammation.* 2017;14:8.
27. Koshimori Y, Ko J-H, Mizrahi R, et al. Imaging striatal microglial activation in patients with Parkinson's disease. *PLoS One.* 2015;10:e0138721.
28. Ouchi Y, Yoshikawa E, Sekine Y, et al. Microglial activation and dopamine terminal loss in early Parkinson's disease. *Ann Neurol.* 2005;57:168–175.
29. Gao Y, Nie K, Huang B, et al. Changes of brain structure in Parkinson's disease patients with mild cognitive impairment analyzed via VBM technology. *Neurosci Lett.* 2017;658:121–132.
30. Mawlawi O, Martinez D, Slifstein M, et al. Imaging human mesolimbic dopamine transmission with positron emission tomography: I. Accuracy and precision of D_2 receptor parameter measurements in ventral striatum. *J Cereb Blood Flow Metab.* 2001;21:1034–1057.
31. Svensson JE, Schain M, Plavén-Sigray P, et al. Validity and reliability of extrastriatal [^{11}C]raclopride binding quantification in the living human brain. *Neuroimage.* 2019;202:116143.
32. Schain M, Zanderigo F, Mann JJJ, Ogden RTT. Estimation of the binding potential BPND without a reference region or blood samples for brain PET studies. *Neuroimage.* 2017;146:121–131.
33. Feng L, Jensen P, Thomsen G, et al. The variability of translocator protein signal in brain and blood of genotyped healthy humans using in vivo ^{123}I-CLINDE SPECT imaging: a test–retest study. *J Nucl Med.* 2017;58:989–995.
34. Kreisl WC, Fujita M, Fujimura Y, et al. Comparison of [^{11}C]-(*R*)-PK 11195 and [^{11}C]PBR28, two radioligands for translocator protein (18 kDa) in human and monkey: implications for positron emission tomographic imaging of this inflammation biomarker. *Neuroimage.* 2010;49:2924–2932.
35. Owen DR, Guo Q, Kalk NJ, et al. Determination of [^{11}C]PBR28 binding potential in vivo: a first human TSPO blocking study. *J Cereb Blood Flow Metab.* 2014;34:989–994.